Dynamic properties of a sand–nanoclay composite

Article *in* Géotechnique · February 2019

DOI: 10.1680/jgeot.18.p.017

5 authors, including:

Felipe Ochoa-Cornejo
University of Chile
24 PUBLICATIONS **36** CITATIONS
SEE PROFILE

Cliff T. Johnston
Purdue University
212 PUBLICATIONS **7,234** CITATIONS
SEE PROFILE

Marika Santagata
Haute école de santé Genève
24 PUBLICATIONS **360** CITATIONS
SEE PROFILE

Dynamic properties of a sand–nanoclay composite

FELIPE OCHOA-CORNEJO*, ANTONIO BOBET†, CLIFF JOHNSTON†, MARIKA SANTAGATA† and JOSEPH V. SINFIELD†

The paper describes the influence of 1–3% (by dry mass of sand) Laponite, a highly plastic synthetic nanoclay, on the dynamic properties of Ottawa sand, based on undrained resonant column tests. The effect of Laponite depends on the amount added, the confining stress and consolidation time. With 1% Laponite, there is an increase in the very small-strain shear stiffness at all confining stresses, which increases with extended consolidation time, reflecting the thixotropic nature of the nanoclay. Added Laponite also produces an increase in small-strain damping, an extension of the linear strain threshold; and it delays the generation of excess pore pressure, degradation of shear modulus and increase in damping with shear strain. These effects, which become more significant with increasing Laponite content, can be attributed to the impact of the clay on the fabric and grain-to-grain contacts. Evidence is provided that Laponite interferes with direct interaction between the sand grains, and the thickness of the clay layer present at the contacts appears to control the small-strain behaviour of the sand–Laponite mixtures. The formation of a gel-like pore fluid from the hydration of Laponite in the voids, and the degree to which it occupies the pore space, are responsible for the behaviour in the non-linear region.

KEYWORDS: dynamics; fabric/structure of soils; liquefaction; particle-scale behaviour; sands; stiffness

INTRODUCTION

Shear modulus (G) and damping ratio (D) are fundamental soil properties that are critical to earthquake engineering, machine and natural vibrations, as well as soil–structure interaction problems. G is related to the stiffness of particle contacts or the velocity of shear waves propagating through the soil skeleton (Viggiani & Atkinson, 1995; Lee *et al*., 2017). D relates to the energy dissipation at the grain contacts level (Cascante & Santamarina, 1996; Wang & Santamarina, 2007; Ham *et al*., 2012). Both parameters are shear strain dependent. At very small strains, the response can be considered linear, with constant values of shear modulus (G_0) and damping (D_0) (e.g. Kokusho, 1980; Wang & Santamarina, 2007). Beyond a limit shear strain, the value of which depends on both soil and testing conditions, G decreases and D increases non-linearly (e.g. Vucetic & Dobry, 1991; Viggiani & Atkinson, 1995; Zhang *et al*., 2005). Several factors influence the dynamic response of soils, including effective stress level, stress history, void ratio, particle morphology, aging, soil structure and composition. In the case of clays it has been long established (e.g. Vucetic & Dobry, 1991) that the primary factor controlling the evolution of G and D in the non-linear region is the soil's plasticity index (PI), with increasing plasticity leading to extension of the initial linear region, and increase in the threshold shear strain, γ_{th}, which delays generation of excess pore pressure and stiffness degradation (e.g. Hsu *et al*., 2007; El Mohtar *et al*., 2014; Dobry & Abdoun, 2015). Plasticity plays a role also in the dynamic response of sands containing fines, as demonstrated by investigations of the behaviour of sands with both non-plastic and plastic fines (e.g. Mancuso *et al*., 2002; Carraro *et al*., 2009; El Mohtar *et al*., 2014). This paper seeks to contribute to this area of research through an experimental study of the dynamic properties of Ottawa sand containing very small amounts (1–3% by dry mass of the sand) of Laponite, a synthetic nanoclay, which, due to its high plasticity (PI > 1000%) has been referred to as a 'super plastic' clay (Ochoa-Cornejo *et al*., 2016). This nanoclay has recently attracted interest for its potential to treat sands susceptible to liquefaction and research has demonstrated its effectiveness in this capacity at least at the laboratory scale (Ochoa-Cornejo *et al*., 2014, 2016; Huang & Wang, 2016). In this context, the experimental work presented in this paper also offers insight into the small-strain mechanisms responsible for the reduced mobility of the sand grains observed in the presence of Laponite in cyclic triaxial tests (Ochoa-Cornejo *et al*., 2014, 2016).

The experimental programme examined in this paper consists of undrained resonant column tests performed on specimens of clean sand, and sand dry-mixed with 1% and 3% of Laponite by dry mass, under similar conditions of skeleton relative density (15–25%), aging duration and effective stress levels. G_0 and D_0 were measured during specimen preparation, consolidation and aging, to describe the small-strain dynamic properties with stress level and time. Degradation curves with strain were also obtained. The results provide insight into the changes in the fabric and the interparticle interactions controlling the response of the soil. Optical microscopy and particle-scale experiments were conducted to complement and support the hypotheses regarding the effect of Laponite on the properties of the sand.

The findings of this work are compared with results obtained by El Mohtar *et al*. (2008, 2013, 2014) for sand specimens with 3% and 5% of bentonite, with the aim of contributing to the development of a general framework describing the effects of highly plastic fines on the dynamic properties and small-strain behaviour of sands.

Manuscript received 21 January 2018; revised manuscript accepted 25 February 2019.
Discussion on this paper is welcomed by the editor.
* University of Chile, Santiago, Chile.
† Purdue University, West Lafayette, IN, USA.

EXPERIMENTAL METHODS

Materials

The experimental programme consisted of undrained resonant column tests performed on specimens of clean

Ottawa sand, and the same sand dry-mixed with Laponite RD, a synthetic layered silicate manufactured by BYK Additives Ltd.

Ottawa sand is a clean (<1% fines), uniform ($C_u = 1{\cdot}5$–$1{\cdot}9$) silica sand with a specific gravity of 2·65, and e_{min} and e_{max} values of 0·48 and 0·78 (El Mohtar, 2008). The particles with diameter between 150 and 850 μm ($D_{10} \sim 0{\cdot}20$ mm, $D_{30} \sim 0{\cdot}26$ mm, $D_{50} \sim 0{\cdot}33$ mm, $D_{60} \sim 0{\cdot}38$ mm) have rounded to subrounded shape (Fig. 1), with sphericity between 0·7 and 0·9, and roundness between 0·5 and 0·7 (Krumbein & Sloss, 1963).

Laponite RD ($Na_{+0{\cdot}7}[(Si_8Mg_{5{\cdot}5}Li_{0{\cdot}3})O_{20}(OH)_4]^{-0{\cdot}7}$), herein referred to as Laponite, consists of disc-shaped nanoparticles. Single Laponite particles have a diameter of ~25 nm and a thickness of 1 nm (Fig. 2(a)), and specific gravity between 2·53 and 2·57 (Kroon *et al.*, 1998; Rockwood Additives, 2008). Laponite powder has a high affinity for water and, in the form in which it is supplied, has a moisture content between 7 and 8% (El Howayek, 2011). Its bulk unit weight is around 10 kN/m^3 (Hou *et al.* (2004) and the present study), with Laponite particles forming stacks that have silt to sand size ($D_{50} = 46$ μm; $D_{90} = 128$ μm; $D_{10} = 5$ μm (BYK Limited, personal communication, 2015)). This is evident in the micrographs presented in Fig. 3, which show silt size aggregates of particles. While the theoretical specific surface area (SSA) of Laponite exceeds 800 m^2/g, values reported in the literature with the Brunauer–Emmett–Teller (BET) technique fall around 400 m^2/g (El Howayek, 2011).

Laponite has a 2 : 1 mineral structure (Fig. 2(b)), similar to that of natural hectorite, with a magnesium trioctahedral sheet sandwiched between two tetrahedral sheets. Isomorphic substitution of magnesium cations (Mg^{2+}) in the central layer by lithium cations (Li^+) causes negatively charged surfaces, with a charge density of −0·014 e/A^2 (Herrera *et al.*, 2004), equivalent to ~1000 charges per

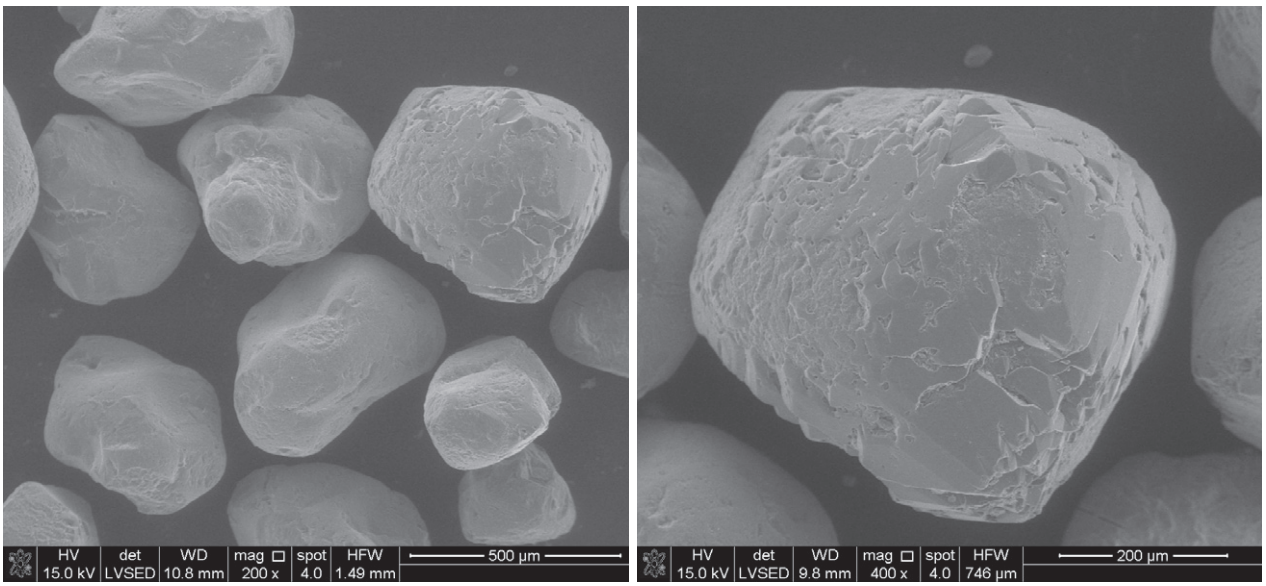

Fig. 1. SEM images of (a) a group of Ottawa sand particles and (b) a single grain taken using FEI Quanta 3D field emission SEM in Purdue University's Life Science Microscopy Facility (operating parameters: 15 kV accelerating voltage, ~10 mm working distance, spot 4 and 30 μm aperture)

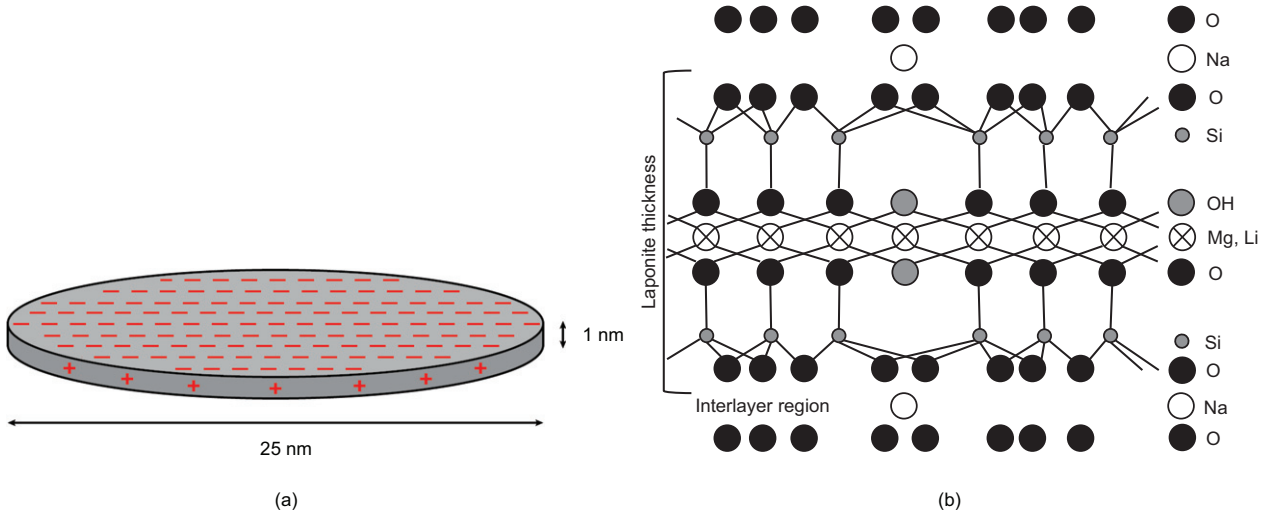

Fig. 2. (a) Schematic representation of a typical Laponite disc particle (modified from Rockwood Additives (2008)) and (b) trioctahedral mineral structure of Laponite

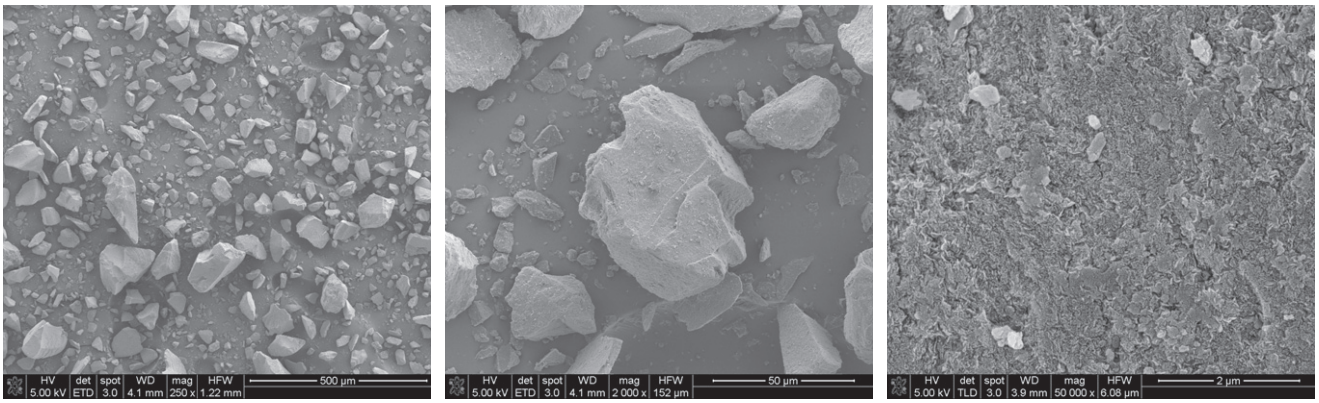

Fig. 3. SEM images of aggregates forming the Laponite powder taken using FEI Quanta 3D field emission SEM in Purdue University's Life Science Microscopy Facility (operating parameters: 15 kV accelerating voltage, ~10 mm working distance, spot 4 and 30 µm aperture)

face. This results in a cation exchange capacity of ~0·95 meq/g. Surface negative charges are electrically counterbalanced by precipitated salts and sodium cations in the interlayer space. Positive charges (~0·9 e/nm, corresponding to ~100 charges) are present on the rims (Joshi *et al.*, 2008).

When dispersed in water at high shear rates, Laponite forms clear, primarily monodisperse dispersions with ~80% of the colloidal particles in an isolated state, and the rest in stacks of two to four particles (Balnois *et al.*, 2003). Owing to their unique rheological properties, these dispersions find application in products such as drilling fluids, detergents, paints, inks and personal care products.

Resonant column apparatus

The Drnevich type resonant column apparatus (Drnevich *et al.*, 1978), in Purdue University's Lyles School of Civil Engineering, was used to evaluate the mechanical response of sand and sand–Laponite specimens at shear strains ranging between 10^{-4}% and about 4×10^{-2}%. The apparatus consists of: the resonant column cell, which houses a specimen 7 cm dia. and 15 cm high, and contains the top cap equipped with four magnets placed inside electrical coils through which torsion is applied to the specimen; a pressure panel for application of cell and back-pressure, and measurement of specimen volume change; sensors for measuring cell pressure, pore pressure, specimen axial deformation and acceleration of the top cap system; hardware for control and data acquisition, including a variable frequency sine-wave oscillator, which provides input to the drive coils, and an oscilloscope used for measuring the resonant frequencies; as well as reading units for the various sensors.

The shear strain, the shear modulus and the damping ratio of the soil are calculated from the torque and the acceleration recorded at the resonant frequency according to ASTM D 4015 (ASTM, 2007). The Drnevich apparatus measures the electrical current passing through the coils, as compared to the voltage drop across the coils. This allows for measuring the actual torque applied to the specimen without the need to correct for the inherent counter electromotive force (EMF effect) generated from the movement of the magnet in the electrical field produced by the coils, which can significantly affect damping measurements (Wang & Santamarina, 2007).

Specimen preparation, testing procedures and testing programme

When preparing sand–Laponite specimens, the sand and the Laponite were first poured in a sealed plastic container and mixed through manual shaking for 20 min. After mixing, the material was dry pluviated inside a triaxial split mould. A similar procedure was followed for clean sand specimens. Air pluviation procedures were calibrated to achieve similar formation skeleton relative densities (D_{rsk}) (when possible between 15 and 25%) for clean sand specimens and specimens with 1% Laponite (see Table 1). The skeleton relative density is calculated based on the skeleton void ratio (which considers that only the sand contributes to the solid phase) and the limiting void ratios (e_{max} and e_{min}) of the clean sand. Values of D_{rsk} in this range could not be achieved with 3% Laponite, even after tapping. For these specimens the formation skeleton void ratio always exceeded the maximum void ratio (e_{max}) of the clean sand, yielding negative values of D_{rsk} (see Table 1).

Following set up, the specimens were flushed first with carbon dioxide and then with deionised de-aired water under a confining stress of approximately 25 kPa, and then back-pressure saturated to 300–350 kPa under constant effective stress, to reach a B value $\geq$0·95. Deionised water was used to ensure that variations in water characteristics did not affect the results, as salinity and pH are known to affect the interaction of Laponite particles.

Following saturation, the specimens were isotropically consolidated to 100 kPa. In a select number of tests, the effective confining stress was further increased to 300 kPa. As a result of the flushing, saturation and consolidation stages the skeleton relative density increased in all specimens. The pre-shear values of D_{rsk} are summarised in Table 1. It can be seen that the most significant increase in D_{rsk} was observed in the specimens with 3% Laponite.

Clean sand specimens were left to age at the maximum confining stress for a minimum of 1 h and a maximum of 74 h, whereas for sand–Laponite specimens the aging duration ranged from approximately 3 days to almost 1 week. The aging duration of 3 days was based on results of rheological tests, which showed that at this time the rheology of the Laponite pore fluid expected to develop in the pore space was similar to those of bentonite dispersions examined in previous work (El Mohtar, 2008).

Measurements of G_0 and D_0 were conducted throughout each test to describe their variation as a function of stress level, void ratio and time. In these measurements, the torque applied is small to ensure that the resulting shear strain γ remains below 0·0005% – that is, well within the linear range of the response. Under these conditions the test probes the 'intact' soil fabric (Cascante & Santamarina, 1996), with no disturbance to the specimen.

Following completion of the aging phase at the maximum confining stresses targeted in each of the tests, cyclic loading

Table 1. Summary of testing programme

Test no.	Laponite: %	Formation e_{sk}	Formation D_{rsk}: %	σ'_{cmax}: kPa	Pre-shear e_{bulk}	Pre-shear e_{sk}	Pre-shear D_{rsk}: %	Aging duration at σ'_{cmax}: h
1	0	0·713	22	100	0·705	0·705	25	1
2	0	0·712	23	300	0·697	0·697	28	3
3	0	0·719	20	100	0·713	0·713	22	6
4	0	0·716	21	100	0·710	0·710	23	10
5	0	0·715	22	100	0·712	0·712	23	29
6	0	0·711	23	100	0·706	0·706	25	74
7	1	0·746	11	100	0·720	0·738	14	74
8	1	0·732	16	100	0·707	0·725	18	74
9	1	0·736	15	100	0·701	0·719	20	77
10	1	0·728	17	100	0·702	0·720	20	86
11	1	0·739	14	100	0·714	0·732	16	88
12	1	0·742	13	100	0·716	0·734	15	165
13	1	0·706	25	300	0·665	0·682	33	74
14	3	0·804	<0*	300	0·705	0·758	7	73
15	3	0·804	<0*	100	0·739	0·793	<0*	73
16	3	0·788	<0*	300	0·705	0·758	7	78

*A negative skeleton relative density reflects the fact that the skeleton void ratio is smaller than the bulk maximum void ratio of the clean sand.

(at resonance) was applied to the specimen under undrained conditions, measuring the excess pore pressure at the base of the specimen. Resonant frequencies ranged between 50 and 150 Hz. The angular amplitudes were such that the shear strains of the soil ranged between 10^{-4} and 3×10^{-2}%, allowing evaluation of the dynamic properties in the linear and non-linear regimes of deformation of the soil.

Table 1 summarises the resonant column testing programme.

SMALL-STRAIN PROPERTIES OF SAND WITH LAPONITE

Dynamic properties at very small strains

Extensive research has been conducted on the factors affecting the initial shear modulus G_0 of soils. As established through both experimental studies and theoretical work based on contact mechanics, G_0 correlates with effective stress confinement, void ratio and overconsolidation ratio (OCR) (Duffy & Mindlin, 1957; Hardin & Black, 1966; Drnevich *et al.*, 1978; Hardin, 1978; Kokusho, 1980; Goddard, 1990; Santagata *et al.*, 2005).

Figure 4(a) shows plots of G_0, as a function of the isotropic effective confinement for clean sand and sand with Laponite. All data were obtained immediately following the end of primary consolidation, and therefore do not reflect any aging effects. As reported for a wide range of geomaterials, there is a power law relationship between G_0 and effective confining stress for both clean sand and sand–Laponite specimens. At any confining stress, the specimens with 1% Laponite exhibit a shear modulus 10–20% higher than that of clean sand. The data for 3% Laponite go from falling below to above the clean sand results as the stress level increases, while remaining below the values measured on the specimens with 1% Laponite. This observation is discussed further below when analysing the data reported in Fig. 5.

The following expression (Hardin, 1978) has been widely used to describe the dependence of G_0 on effective confining stress, void ratio and OCR

$$G_0 = C_g \times \mathrm{OCR}^k \times F(e) P_a^{1-n} \sigma_0'^n \quad (1)$$

where C_g is an intrinsic soil constant that depends on particle nature and fabric; OCR is the overconsolidation ratio (equal to 1 for all tests performed in this study); $F(e)$ is a void ratio function; P_a is the atmospheric pressure used as a reference stress; and the coefficients k and n are parameters that depend on the characteristics of the soil (e.g. plasticity) and the nature of the contacts between the soil particles (Sawangsuriya, 2012). The following void ratio function, proposed by Hardin (1978) and applicable to void ratios between 0·4 and 1·2, can be used to normalise G_0 to account for differences in the void ratio

$$F(e) = \frac{1}{0{\cdot}3 + 0{\cdot}7e^2} \quad (2)$$

Figure 4(b) shows that once differences in the bulk void ratio are accounted for, the relative position of the three curves remains unchanged.

Figure 5 plots the initial normalised shear modulus as a function of Laponite percentage, separating the data based on stress level. At the three stress levels examined, the normalised shear modulus of the sand with 1% Laponite exceeds the values measured on the clean sand. With 3% Laponite, the normalised shear modulus falls below the clean sand data at 25 and 100 kPa but exceeds the value measured on the clean sand at 300 kPa, approaching the results for 1% Laponite. These observations differ from previous experimental evidence showing that the presence of fines – both plastic and non-plastic – reduces the shear stiffness and that the reduction is more pronounced as the fine content increases (Iwasaki & Tatsuoka, 1977; Salgado *et al.*, 2000; Lee *et al.*, 2004; El Mohtar *et al.*, 2008; Carraro *et al.*, 2009).

It is hypothesised that, while in all cases Laponite interferes with the contacts between the sand grains, the amount of Laponite trapped at the contacts controls the effect on the small-strain shear modulus. When the Laponite 'layer' is sufficiently small (i.e. with 1% Laponite, or after consolidation of the 3% Laponite specimen to 300 kPa), the modulus is increased, suggesting that Laponite provides bonding/bridging at the particle contacts. With 3% Laponite at confining stress $\leq$100 kPa, the effect of the thicker clay layer is that of softening the response. While the thickness of the Laponite layer present at the grain contacts was not directly measured, it is inversely related to the skeleton relative density, which, as summarised in Table 1, decreases with increasing confining stress and decreasing Laponite content.

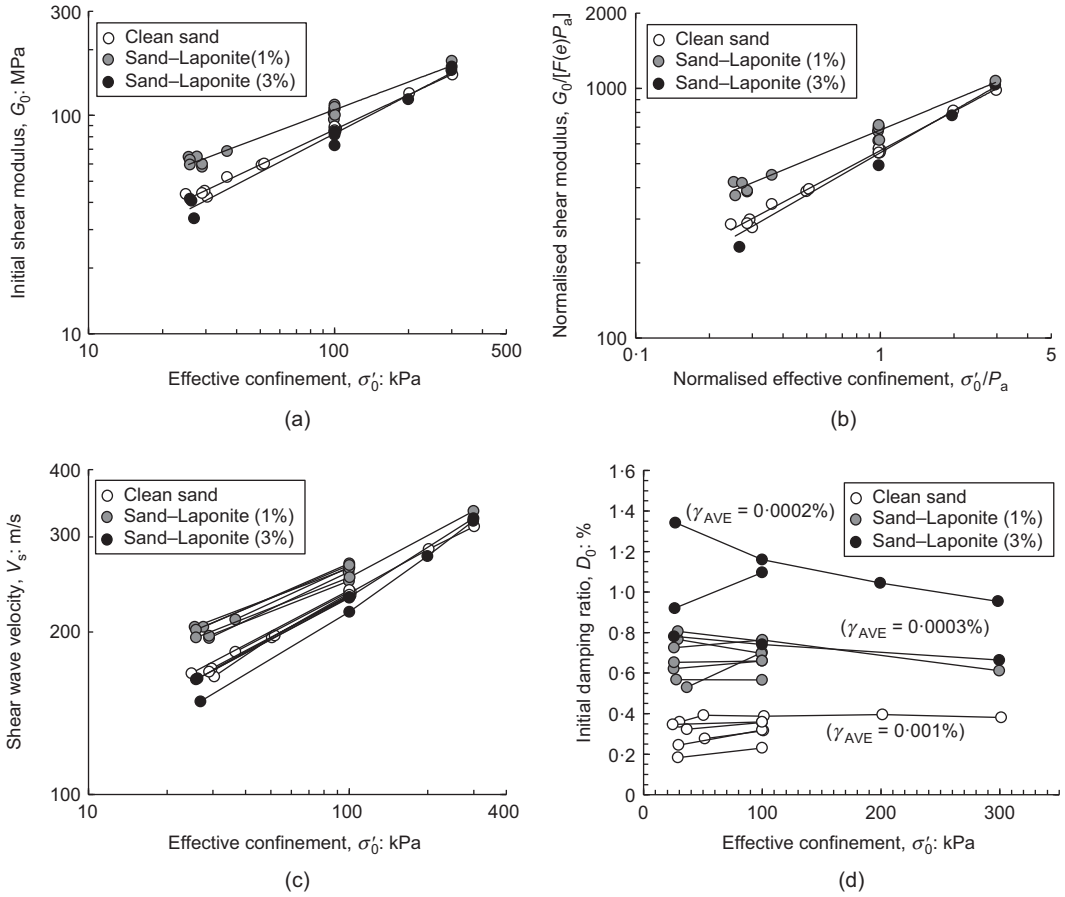

Fig. 4. (a) Initial shear modulus, (b) normalised shear modulus, (c) shear wave velocity and (d) damping ratio of clean sand and sand with Laponite as a function of effective stress

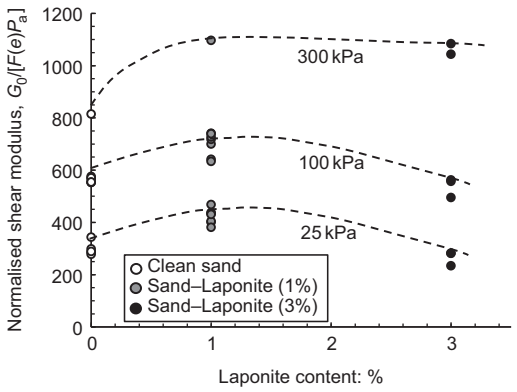

Fig. 5. Effect of Laponite percentage on the normalised initial shear modulus at 25, 100 and 300 kPa (G_0 normalised by the bulk void ratio)

G_0 is related to V_s, the velocity of the shear wave propagating through the interparticle contacts of the soil, through the following equation

$$G_0 = \rho V_s^2 \tag{3}$$

where ρ is the soil's total density.

As for G_0, and in agreement with previous studies on granular materials (Cho *et al.*, 2006; Sawangsuriya *et al.*, 2007), there is a power law relationship (Fig. 4(c)) between V_s and the effective confining stress of the type

$$V_s = \alpha(\sigma'_0/p_r)^{\beta} \tag{4}$$

where p_r is a reference stress.

As also seen for G_0, specimens with 1% Laponite present higher V_s with respect to clean sands. The difference, 5–20% over the stress range investigated, decreases with effective confining stress.

Figure 4(d) presents the values of the small-strain damping ratio, D_0. Measuring damping at very small strains presents some challenges, as apparatus properties can come into play. All D_0 data presented here, as well as the results for sand–bentonite specimens referred to in a later section (entitled 'Comparison to experimental results for sand–bentonite specimens'), were performed with the same device, using nearly identical calibrations and procedures. As a result, they provide an accurate representation of the relative damping behaviour of these geomaterials and can be used to assess the influence of the amount and type of fines present in the sand matrix.

For clean sand D_0 falls between 0·2 and 0·4%, consistent with literature data for clean sands (Wang & Santamarina, 2007). The sand–Laponite specimens present higher D_0, which increases with the Laponite percentage. The differences between the three data sets are small but consistent, especially since the strain range over which D_0 was measured on the sand–Laponite specimens is smaller than for clean sand (see Fig. 4(d)). It is suggested that the higher D_0 for sand–Laponite specimens reflects a viscous damping contribution from the presence of Laponite at the sand grain contacts: the greater the amount of Laponite trapped at the contacts, the greater the increase in damping. A similar effect has been reported for artificially cemented sands (Saxena *et al.*, 1987) at low cementation levels when the cement particles coat the areas of the contacts between the originally clean sand grains.

The effect of confining stress on D_0 is best elucidated examining the data from tests in which measurements were conducted at various stress levels on the same specimen. For clean sand it appears that in the 25–300 kPa stress range examined there is no significant variation in D_0 with stress level. This is expected, as it has been shown that in sands small-strain damping in soils is non-frictional (Wang & Santamarina, 2007). For most of the tests conducted on specimens with 1% Laponite, D_0 shows limited variation between 25 and 100 kPa. However, in the single test in which measurements were conducted up to 300 kPa, the data indicate a decrease of D_0 at the highest confinement. With 3% Laponite, based on the two tests in which measurements of damping were made at stress levels between 25 and 300 kPa, there is a continuous reduction in D_0 with confining stress. These trends indicate an evolution of the interparticle contacts with stress level, attributed to the compression and/or extrusion of the clay layer created between the grains during specimen preparation, with a resulting decrease of the viscous damping. This effect is more significant with 3% Laponite, owing to the greater amount of clay potentially present at the contacts.

Variation of the dynamic properties with shear strain

Extensive experimental work on a variety of soils has shown that beyond $\gamma \sim 10^{-3}\%$ there is a marked reduction of G and an increase in D with shear strain. These trends reflect the occurrence of grain contact slippage and particle rearrangement (e.g. Vucetic & Dobry, 1991; Viggiani & Atkinson, 1995; Vucetic *et al*., 1998; El Mohtar *et al*., 2013).

The shear phase conducted at the end of each of the tests identified in Table 1 provides the means to understand the effects of Laponite on the small-strain non-linearity. This last part of the tests was performed after completion of the aging stage, which for specimens with Laponite, extended to at least 72 h after the end of primary consolidation. Shear strains during this stage ranged between $10^{-4}\%$, a state of 'intact' soil fabric (Cascante & Santamarina, 1996), and $\sim 4 \times 10^{-2}\%$, where deformations and relative motion of the grains become significant (Santamarina *et al*., 2001).

Figure 6 shows plots of G, D, G/G_0 and $\Delta u/\sigma'_0$ against shear strain from tests conducted at 100 kPa. Fig. 6(a) shows that the shear modulus of the specimens with Laponite is higher than that of clean sand over the entire shear strain range probed by the tests. The results for 3% Laponite fall below those for 1% Laponite at small strains, and slightly exceed them beyond ~0·015% shear strain. Owing to the effects of aging, the values of G_0 measured on the sand–Laponite specimens exceed the values shown in Figs 4 and 5. In particular, for the specimens with 3% Laponite, the values of G_0 measured at 72 h no longer fall below the data for the clean sand (see additional discussion on the increase in G_0 with time in the next section 'Time dependence of the dynamic properties').

When plotted normalised by G_0 measured at the start of the shear stage (Fig. 6(c)), the data highlight how the three soil types all have a similar response, with a virtually constant value of G up to approximately $10^{-3}\%$, and similar modulus reduction up to a shear strain of $3 \times 10^{-3}\%$. For higher strains, the curves diverge, with the clean sand exhibiting the most significant degradation, followed by the specimens with 1% and 3% Laponite, respectively (e.g. for $\gamma = 10^{-2}\%$, $G/G_0 = 0{\cdot}6$–$0{\cdot}65$ for clean sand as opposed to 0·7–0·8 for the sand–Laponite specimens).

Given that the tests were performed undrained, excess pore pressure was generated within the specimens. The resulting effective stress loss is, in part, responsible for the modulus degradation observed with increasing shear strain. As shown in Fig. 6(d), $\Delta u/\sigma'_0$ is zero in the small-strain regime of deformation and rises rapidly beyond a certain threshold shear strain. The presence of Laponite leads to

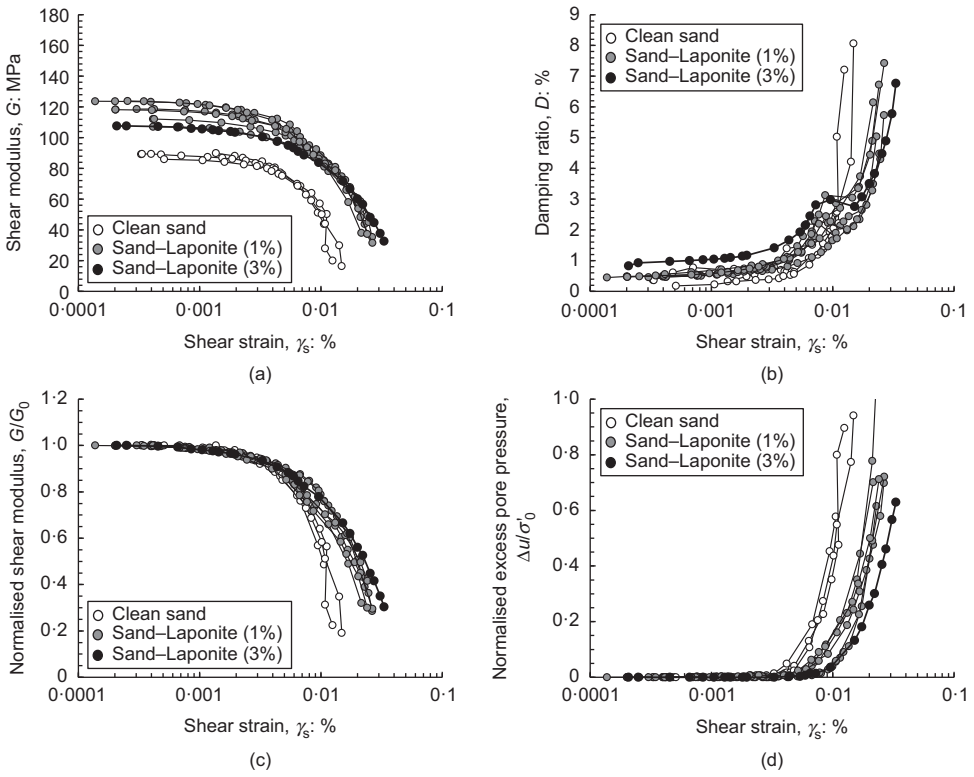

Fig. 6. Variation of (a) shear modulus, (b) damping, (c) normalised shear modulus and (d) normalised excess pore pressure of clean sand and sand with Laponite, as a function of shear strain (tests at $\sigma'_0 = 100$ kPa)

an increase in this threshold (from $\sim 3 \times 10^{-3}\%$ for clean sand to $5–7 \times 10^{-3}\%$ for the sand–Laponite specimens) and a reduced excess pore pressure at any shear strain (e.g. at $10^{-2}\%$ $\Delta u/\sigma_0' \sim 0{\cdot}35–0{\cdot}5$ for clean sand, as opposed to $\Delta u/\sigma_0' \sim 0{\cdot}05–0{\cdot}15$ and $\Delta u/\sigma_0' < 0{\cdot}05$ for specimens with 1% and 3% Laponite, respectively). For all the materials, the threshold strain level is higher than the shear strain corresponding to the onset of non-linearity, signifying that a mechanism, other than the reduction in effective stress driven by the generation of excess pore pressure, contributes to the shear modulus degradation and, in particular, controls the modulus reduction at very small strains.

Based on analysis of the cyclic triaxial response of sand specimens with different percentages of Laponite identical to those examined in this work, Ochoa-Cornejo *et al.* (2016) propose that the reduced mobility of the sand particles in sand–Laponite specimens can be ascribed to: (*a*) bonding/bridging at the sand particle contacts due to the presence of the plastic fines; and (*b*) the restraint provided by the pore fluid formed as a result of the hydration of the clay present in the pore space. As shown by El Howayek *et al.* (2014) the structure of the gel-like pore fluid that is formed under these conditions is similar to that of concentrated Laponite dispersions, which exhibit solid-like (elastic) behaviour over a broad range of strains (e.g. see Santagata *et al.*, 2014). Cryo-scanning electron microscopy (SEM) images presented by El Howayek *et al.* (2014) show the presence of water 'pockets' within the pore space – evidence that the Laponite gel is not continuous.

Similarly to what is suggested by Ochoa-Cornejo *et al.* (2016) to explain differences in cyclic behaviour between the different specimens, it is hypothesised that the second mechanism is enabled with higher percentages of Laponite, leading to continued particle restraint, and thus reduced excess pore pressure generation, and shear stiffness degradation with increasing shear strain.

Figure 6(b) presents the damping ratio results. For all specimens, D is relatively constant for shear strains ranging between 10^{-4} and $10^{-3}\%$. The values measured in this region fall in the 0·2–1% range depending on the material (for the sand–Laponite specimens they are smaller than the values in Fig. 4(d) due to the effects of aging – see the next section 'Time dependence of the dynamic properties'). For all specimens, D increases with strain.

In clean sands, the increase in D with strain reflects primarily the increased frictional energy dissipating due to the relative motion of particles and the grinding of the asperities (Richart *et al.*, 1970; Santamarina *et al.*, 2001). In sand–Laponite specimens, additional contributions to damping may come from the breakage of the clay 'connections' between the sand grains, as well as from the viscous pore fluid formed in the pore space as a result of the hydration of the clay fines. This effect has been documented in previous studies (Ellis *et al.*, 2000; Qiu, 2010). The existence of more mechanisms potentially responsible for energy dissipation suggests that larger damping should be expected in specimens with Laponite. This is the case up to $\gamma \sim 0{\cdot}07–0{\cdot}01\%$. However, at larger strains a larger D is measured in the clean sand relative to the sand–Laponite specimens. It is hypothesised that this is a reflection of the lubricating action of the clay at the contacts, which minimises the contribution to the overall damping coming from frictional interactions. The data suggest that the greater the amount of Laponite, the greater the reduction in frictional energy dissipation. Note also that in all the tests the shear strain at which the damping ratio begins to increase is smaller than the strain levels in correspondence to which excess pore pressure is measured. This suggests that energy dissipation associated with frictional interactions as the particles initiate relative motion occurs before any excess pore pressure is developed.

Similar trends with Laponite percentage are observed at a confining stress of 300 kPa (Fig. 7). As expected, relative to 100 kPa, these curves for each soil type show a reduced stiffness degradation, more delayed pore pressure generation and less significant increase in D (not shown) with increasing shear strain. Additionally, the curves for 3% Laponite lie much closer to those for 1% Laponite.

Time dependence of the dynamic properties

Analysis of the consolidation stage of the resonant column tests (including select tests in which only single drainage was allowed to measure the dissipation of excess pore pressure) indicates that, in both clean sand specimens and specimens with Laponite, this process occurs fairly quickly (e.g. consolidation from 25 kPa to 100 kPa occurs in less than 10 s for all specimens).

Measurements of G_0 and D_0 were performed on the soil specimens during the aging period. Consistent with what has been observed for a variety of soils, the specimens with Laponite exhibit behaviour characterised by continuous positive axial and volumetric strains resulting from creep, a steady increase in G_0 and a decrease in D_0. For the durations of aging examined, these effects are close to negligible for clean sand. This is shown in Fig. 8, which plots the ratio of the small-strain shear modulus, $G_{0\text{ref}}$, over the value of G_0 at the end of primary consolidation (these are the values shown in Figs 4 and 5) against time, for specimens consolidated to 100 kPa.

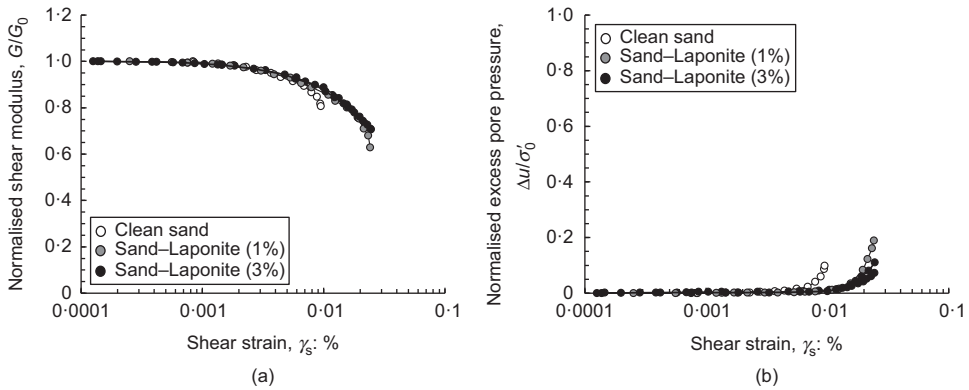

Fig. 7. Variation of (a) normalised shear modulus and (b) normalised excess pore pressure of clean sand and sand with Laponite, as a function of shear strain (tests at $\sigma_0' = 300$ kPa)

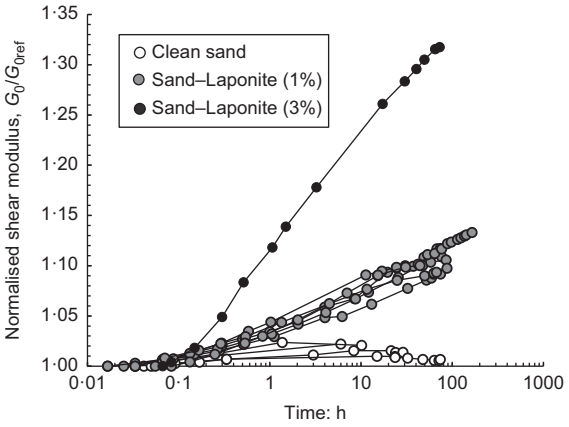

Fig. 8. Variation with time of G_0 normalised by value at reference time (tests at $\sigma'_0 = 100$)

While for the clean sand G_0 exhibits only a small increase over time (<2%, consistent with observations for the same sand at the same confining stress by Wang & Tsui (2009)) over the aging period examined, the modulus increases by 10–12% with 1% Laponite, and by more than 30% with 3% Laponite. As a result, at the end of the aging stage, the 'gap' between the 1% Laponite and the 3% Laponite G_0 values closes. For example, after 72 h at 100 kPa the average G_0 for sand with 3% Laponite is equal to 108 kPa, as opposed to 117 kPa for 1% Laponite (Fig. 6(a)). This is an 8% difference, compared to the 24% difference existing at the end of consolidation (Fig. 4(a)).

Analysis of the data shows that, for aging beyond ~10–15 min, the gain in G_0 is nearly linear with the logarithmic scale of time. This behaviour has been widely documented in the literature (e.g. Anderson & Woods, 1976; Anderson & Stokoe, 1978; Bowman & Soga, 2003). Anderson & Stokoe (1978) proposed that the increase in shear modulus associated with aging can be quantified through the soil-dependent aging coefficient (N_G), defined as

$$N_G = \frac{\Delta G_0}{G_{0(t=t_0)} \log(t/t_0)} \quad (5)$$

where ΔG_0 is the change in shear modulus; $G_{0(t=t_0)}$ is G_0 at the time t_0 where G/G_0 starts to increase linearly with the logarithmic of time. Clean sands typically have $N_G < 3\%$ (Anderson & Stokoe, 1978), whereas for clays N_G is reported to depend on plasticity and stress history and typically falls between 5 and 25% (Santagata & Kang, 2007), evidence of the thixotropic behaviour of these soils.

Values of N_G for the tests shown in Fig. 8 were determined using t_0 of approximately 15 min. Their average values are less than 0·5, ~3·5 and ~10·5% for clean sand, sand with 1% Laponite and sand with 3% Laponite, respectively. Although the value for 1% Laponite is below data reported for clays, the value obtained with 3% Laponite is in the range typical of clays. This suggests that at this stress level the clay layer present at the sand grain contacts is thick enough to control the creep response of the specimen. The values of N_G calculated for clean sand, and sand with 1% and 3% Laponite, are also consistent with the values of the creep coefficient ($C_{\alpha\varepsilon} \sim 0{\cdot}0002$, 0·002 and 0·0046, respectively) derived from the aging stage, in agreement with the reported correlation between these two parameters (Schmertmann, 1991; Lo Presti *et al.*, 1996).

The increase in G_0 measured during aging cannot be solely ascribed to the reduction in void ratio occurring as a result of creep. For example, in the case of sand with 1% Laponite consolidated to 100 kPa, the increase in G_0 is ten times the value that would be predicted using equations (1) and (2), based on the change in void ratio. This demonstrates that, as already well established in the literature, particle densification does not control the increase in G_0 with aging, which instead has been ascribed to both mechanical (e.g. stress state changes, particle rotation and local rearrangement, as well as static fatigue effects) and physicochemical processes (e.g. mineral precipitation, ion accumulation at mineral surfaces) (Schmertmann, 1991; Nakagawa *et al.*, 1995; Bowman & Soga, 2003; Baxter & Mitchell, 2004; Michalowski & Nadukuru, 2012). In clays both play a role, and together determine the thixotropic nature of these soils.

At 300 kPa N_G decreases slightly (from 3·5 to 2·3%) in the specimens with 1% Laponite, while the decrease is very significant – ~10·5 to around 4% – with 3% Laponite, falling below the data for clays. This supports the hypothesis that, as the stress increases, the clay present at the particle contacts is compressed and/or squeezed out.

Figure 9 shows the variation in D_0 normalised by the value at the end of consolidation over the aging period for clean sands and sand with 1% and 3% Laponite. Again, the data reported are normalised by the value measured at the end of consolidation. Except for one test, over the period probed in the experiments, D_0 of the clean sand shows no significant effect of aging. There is no apparent reason for the different behaviour observed in one of the tests with clean sand. As a note, this is the test characterised by the smallest values of D_0 (which goes from 0·22% at 5 min to 0·18% at 74 h).

A reduction in D_0 is, instead, consistently observed for sand with Laponite, with a nearly linear trend with the logarithmic scale of time, similar to the thixotropic increase of G_0. This is consistent with the more limited data available in the literature on the effects of time on this property (see Marcuson & Wahls, 1978; Lo Presti *et al.*, 1996, 1997; Wang & Tsui, 2009) where the effect of aging was specifically investigated, as well as the effect of the number of cycles on damping. Unlike what was observed for G_0, a greater change in D_0 with aging is observed in the specimens with 1% Laponite (20–35% reduction in D_0 relative to the measurement at the start of the aging) compared to the specimens with 3% Laponite (<8% reduction in D_0 relative to the start of the aging); as a result, in contrast to what was found for G_0, the difference in damping ratio between the two data sets increases with aging. Stiffening of the soil leads to a reduction in damping, and the data for the two tests with 3% Laponite indicate that the change in damping measured in these specimens is on the order of what would be expected from the increase in G_0. However, with 1% Laponite, the

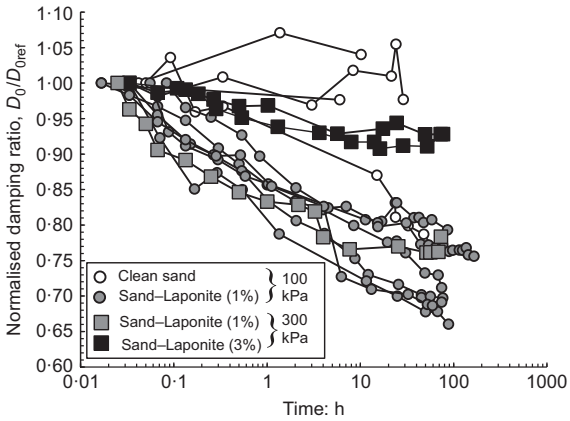

Fig. 9. Variation with time of D_0 normalised by value at reference time

measured reduction in D_0 (27% ± 5% for the seven tests shown) is much greater than what was predicted (9·5% ± 1·6%) from the increase in G_0. This is consistent with the observation by Wang & Tsui (2009: p. 264) that 'aging lessens the damping ratio not only by stiffening the sand samples but also by reducing the energy loss'. This suggests that the primary mechanism responsible for the reduction in damping in these two geomaterials is not the same.

DISCUSSION

Study of sand–Laponite interactions

Hypotheses were made above on the fabric of the specimens and the potential interactions between their components. In this section, some custom experiments that were performed to support these hypotheses are discussed.

Limiting void ratios of sand–Laponite mixtures. Determination of the limiting void ratios of clean Ottawa sand and the same sand mixed with Laponite (0–10%) was performed using method 1A and method A as outlined in ASTM D 4253-16 (ASTM, 2016a) and ASTM D 4254-16 (ASTM, 2016b). The resulting bulk e_{min} and e_{max} and skeleton e_{min} and e_{max} are summarised in Fig. 10. Calculation of the skeleton e_{min} and e_{max} is based on assuming that only the sand grains contribute to the volume of the solids, while the volume of the voids includes the volume occupied by the Laponite.

Both $e_{minbulk}$ and $e_{maxbulk}$ show the same trend with Laponite content. First, with the addition of 1% Laponite, both increase, reflecting that at least part of this small amount of Laponite added positions itself at the sand grain contacts, playing an active role of 'separator' (Thevanayagam *et al.*, 2002). Also, the skeleton void ratios exceed the reference values determined on the clean sand. Moreover, the fact that this is observed for both $e_{minbulk}$ and $e_{maxbulk}$ reflects that the separation survives the vibration process required for measurement of e_{min}, an indication of the high affinity, at least in dry conditions, between Laponite powder and the sand surface.

When the Laponite content is increased to 3%, both $e_{minbulk}$ and $e_{maxbulk}$ decrease, but remain larger than the values for clean sand. With additional Laponite, $e_{minbulk}$ and $e_{maxbulk}$ steadily decrease, while e_{minsk} and e_{maxsk} increase. This indicates that with the further addition of Laponite two things happen: Laponite separates the grains further (reflected in the increase of e_{minsk} and e_{maxsk}), but also starts to fill the void space. Three per cent Laponite is required for the second effect to drive a reduction in $e_{minbulk}$ and $e_{maxbulk}$.

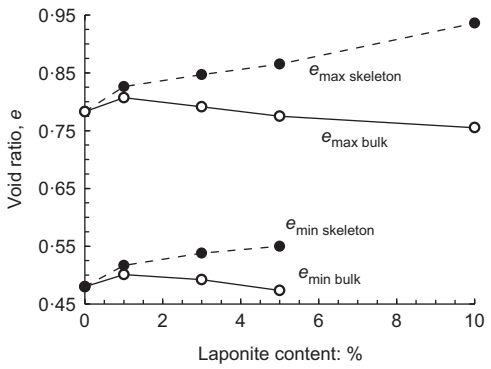

Fig. 10. Variation of the skeleton and bulk e_{min} and e_{max} with Laponite content

Overall, the above findings suggest that the interactions (electrostatic attraction, adhesion, etc.) between Laponite and the sand surface control the packing behaviour of sand–Laponite mixtures. This explains why even minimal Laponite contents (1%) interfere with direct interparticle contacts, and why the trends in the limiting void ratios for the mixtures of sand and silt size aggregates of Laponite shown in Fig. 10 are closer to those reported for sand–clay mixtures (Ovando-Shelley & Pérez, 1997) rather than to those described for sand–silt mixtures (Carraro *et al.*, 2009).

Observations using optical microscopy. Fabric observations and simple micromechanical experiments under completely dry conditions, conducted using an Omano optical microscope equipped with a Optixcam Summit 3.0 camera available in the Pankow Lab of Purdue University's School of Civil Engineering, provide support to some of the hypotheses put forth earlier in this paper. These experiments, which are illustrated in Figs 11–13, are directly relevant to the fabric that is formed under dry conditions during specimen preparation. At this point, their results cannot be extrapolated to wet conditions as those existing after flushing of the specimens with water.

In the first experiment (Fig. 11), a single clean dry sand particle, glued to the tip of a push pin, was lowered onto a surface covered with dry Laponite powder. As shown in the last image, when the particle was lifted, it was covered by Laponite aggregates, providing evidence of the adhesion between the sand surface and the Laponite powder. Along with the above-described increase in $e_{minbulk}$ and $e_{maxbulk}$, this supports the hypothesis that during specimen formation Laponite is trapped at the particle contacts and that, even following vibration, it may not be removed.

This is also highlighted in the images taken looking up at the bottom of a transparent container in which clean sand (Fig. 12(a)) and sand with 1% Laponite (Fig. 12(b)) were pluviated. The image for clean sand shows clear grain–grain contacts and chain forces – evidence of the load-bearing skeleton. The second image for sand with 1% Laponite shows that Laponite aggregates/particles are positioned between the grains and are not fully hosted in the pore space.

Figure 13 illustrates the second part of the experiment shown in Fig. 11. The first image shows a sand particle with Laponite adhering to it (similar to the third image in Fig. 11). In the second image, this sand particle is lowered onto a bed of clean and dry sand grains. The last two images show that, when the grain is lifted, it carries attached to it two additional sand grains. This observation highlights that the adhesion between sand and Laponite is large enough to sustain the weight of a sand particle, at least under dry conditions. Without further investigation, it is not possible, however, to assume that a similar interaction between sand and Laponite exists in the presence of water.

Further evidence of the presence of Laponite in between the sand grains comes from images collected on air-dried samples from a specimen of sand with 1% Laponite, following completion of a resonant column test (Fig. 14). These images show particles bonded/bridged together by Laponite, with the larger aggregates of Laponite for the most part no longer visible, evidence that saturation with water can disperse at least to some degree the Laponite particles. While clearly also reflecting the impact of the drying process, these images provide some preliminary evidence of the bonding/bridging action provided by the Laponite in the saturated specimens, which is reflected, for example, in the increase in G_0 relative to the clean sand.

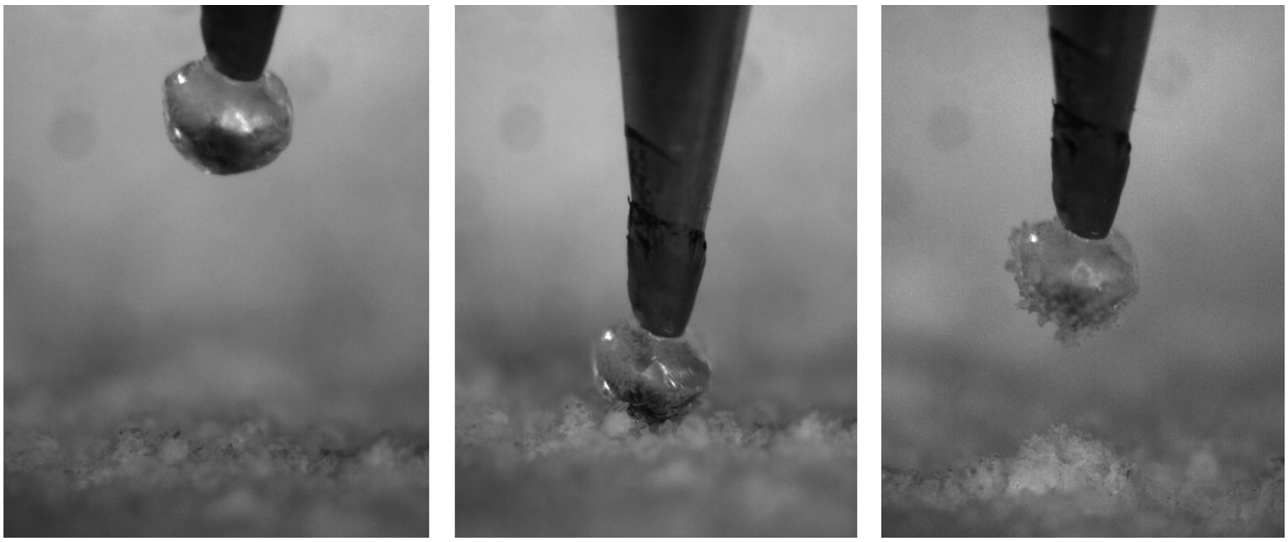

Fig. 11. Sand grain picking up Laponite particles (sand grain is glued to a push pin)

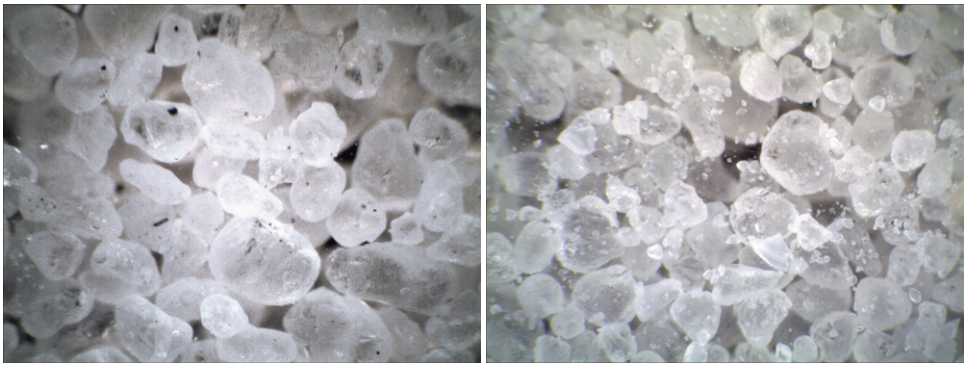

Fig. 12. Initial fabric of (a) clean sand and (b) sand with 1% Laponite

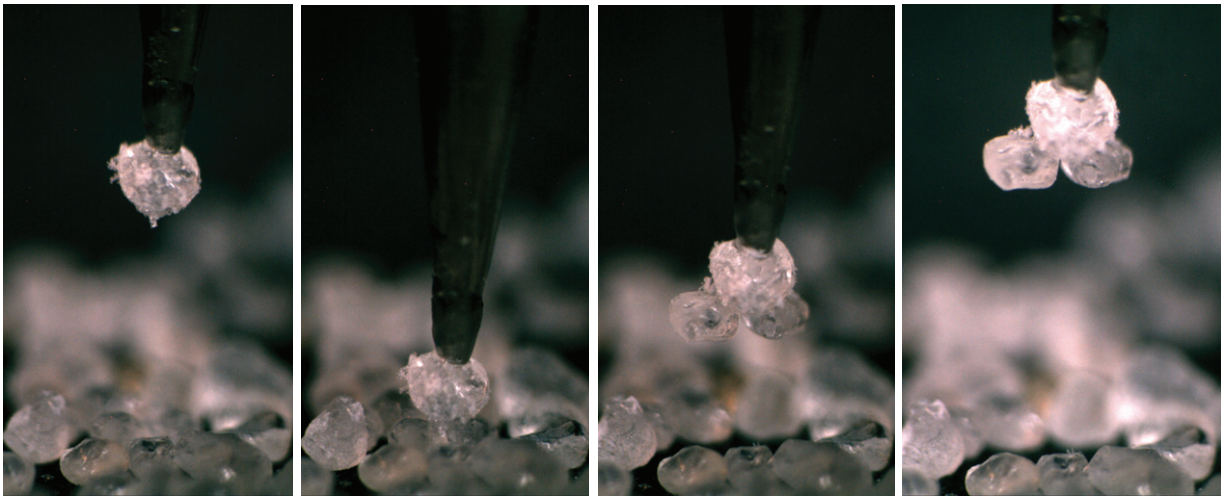

Fig. 13. Sand with Laponite picking up two sand grains

Comparison to experimental results for sand–bentonite specimens

Previous studies have addressed the effect of bentonite on the mechanical response of sands (Gratchev *et al*., 2006, 2007; El Mohtar *et al*., 2013, 2014). In particular, the study by El Mohtar *et al*. (2008, 2013, 2014) was conducted under conditions very similar to those employed in this research, as it comprised undrained resonant column tests performed on dry-mixed specimens of Ottawa sand with 3% and 5% of bentonite (by dry mass of the sand). One difference is in the

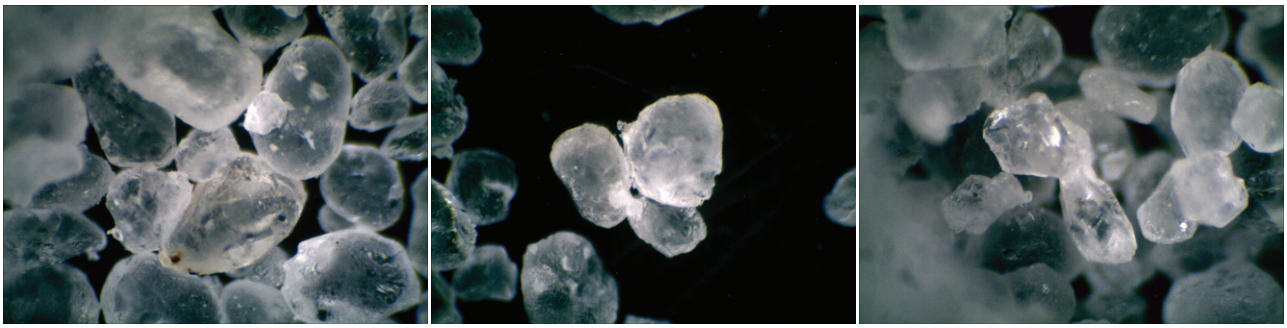

Fig. 14. Evidence of sand particles bonded together by the Laponite from post-testing observations of air-dried sand–Laponite mixtures

slightly higher values of skeleton relative density (30 to 40%) targeted in the tests with bentonite. An additional difference in the testing procedures is that, following flushing with water and before back-pressure saturation, the specimens were left at rest for 72 h to allow the bentonite to swell and hydrate within the sand matrix.

Bentonite consists primarily of smectite-type minerals and thus has mineralogy similar to Laponite. Its particle size is one order of magnitude greater than an individual Laponite particle, although smaller than the size of the aggregates forming the Laponite powder used in this research. While still highly plastic (plasticity index, PI $\sim$ 356% for the sample used in El Mohtar *et al.* (2008, 2013, 2014)), bentonite is significantly less plastic than Laponite (PI $>$ 1000%). As a result, comparing the information obtained by this study to the data obtained in El Mohtar *et al.* (2008, 2013, 2014) can aid in understanding the role played by highly plastic fines on the dynamic response of sands. Moreover, the comparison can provide further insight into the fabric formed in sand–clay mixtures and the quality of the interparticle contacts.

At small strains the two data sets present commonalities, as well as differences. Contrary to what is observed for sand–Laponite specimens, values of the normalised shear modulus (Fig. 15(a)) of the sand–bentonite specimens represent the lower band of the data plotted, falling below the clean sand data over the entire stress range examined. This result, which is ascribed by El Mohtar *et al.* (2008: p. 249) to 'the thin layer of more compressible clay trapped between the sand grains' during the dry-mixing specimen preparation procedure, is in agreement with previous studies on the effect of fines on G_0 (e.g. Hardin & Dmevich, 1972; Hardin, 1978; Lee *et al.*, 2004; Carraro *et al.*, 2009).

A consistent picture of the effect of plastic fines emerges from the D_0 results (Fig. 15(b)). Relative to the clean sand data, which represent the lower end of the measured values and exhibit no significant variation with stress level, the addition of plastic fines leads to an increase in D_0 at any stress level. The effect increases with the percentage of fines, with Laponite having a greater impact than bentonite (e.g. with 3% Laponite D_0 exceeds the values measured with 3% and 5% bentonite). Possible reasons are the higher plasticity of Laponite and/or the greater amount of fines actually present at the contacts (rather than in the pore space). The latter hypothesis is supported by recent comparisons of the limiting void ratios in sand–Laponite and sand–bentonite mixtures (Getchell, personal communication, 2017).

For a given plastic fine, the greater its dosage, the greater the sensitivity of D_0 to stress changes, likely reflecting the compression and/or extrusion of the clay trapped at the sand contacts. At 300 kPa, with 3% bentonite, D_0 is 0·39%, close to the value (0·32%) measured on the clean sand prepared at a similar relative density, and suggesting that the sand grains are close to re-establishing 'direct' contact. This is not the case with either 3% or 1% Laponite, pointing to a stronger adhesion between Laponite and the sand surface, compared to bentonite.

In the non-linear region, El Mohtar *et al.* (2013, 2014) report observations similar to those summarised earlier for Laponite. Specifically, the addition of bentonite extends the linear threshold and the threshold shear strain at which excess pore pressure is triggered, and reduces stiffness degradation (Figs 16(a) and 16(b)). These effects are slightly more significant than what is observed with Laponite. These results are consistent with the hypothesis put forth by Ochoa-Cornejo *et al.* (2016, 2017) that, as the percentage of fines present in the pore space increases, the solid-like gel formed as a result of the hydration of the clay provides an increasing contribution to particle restraint.

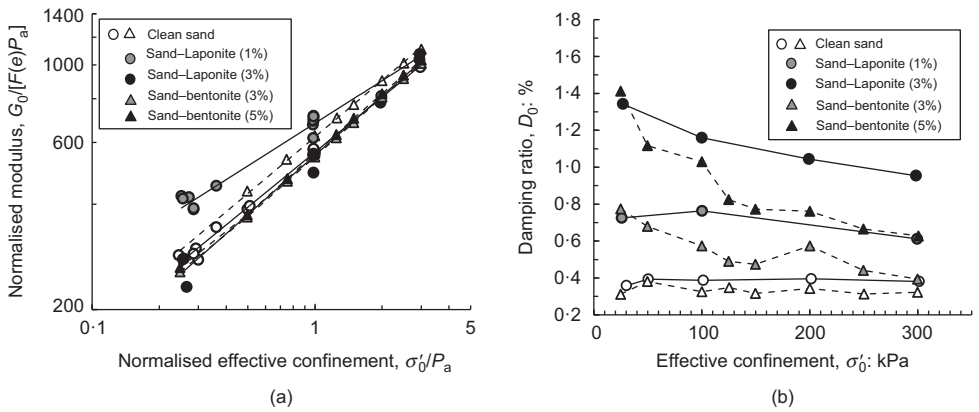

Fig. 15. Initial (a) normalised shear modulus and (b) damping ratio of clean sand, sand with Laponite and sand with bentonite as a function of effective stress (bentonite data from El Mohtar (2008))

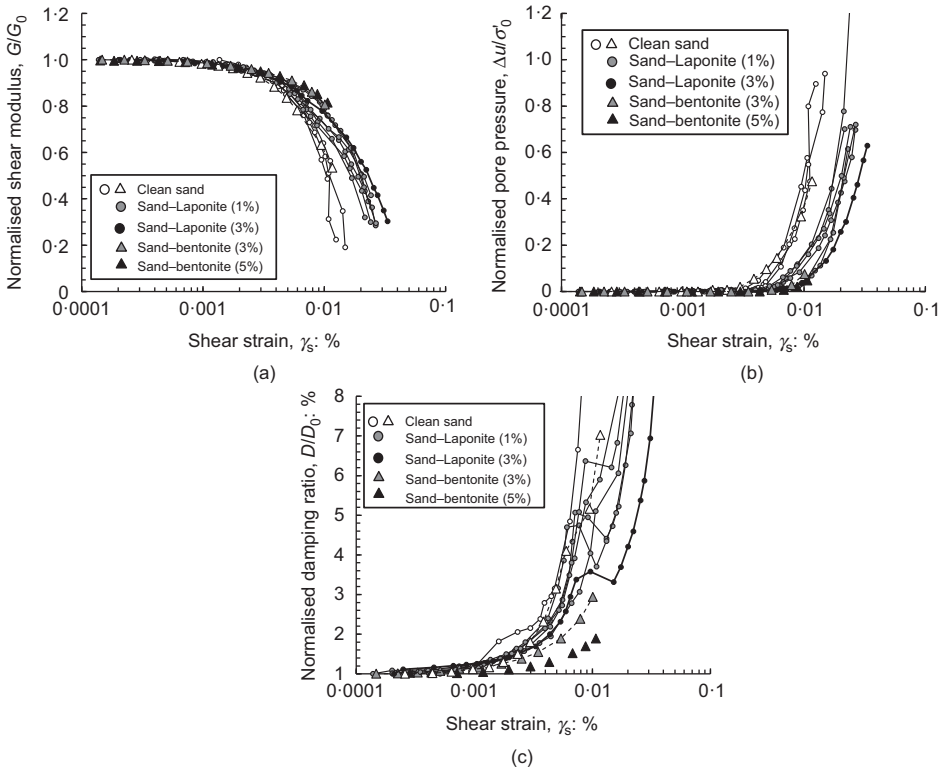

Fig. 16. Variation of normalised (a) shear modulus, (b) excess pore pressure and (c) damping ratio of clean sand, sand with Laponite and sand with bentonite as a function of shear strain (tests at $\sigma'_0 = 100$ kPa, bentonite data from El Mohtar (2008))

Also similar to what was observed for Laponite, the presence of bentonite retards the increase in D with shear strain (Fig. 16(c)). The slowest increase in D is seen with 5% bentonite, a reflection that the higher dosage of fines limits the particle-to-particle frictional interactions responsible for damping at higher strains.

Another element of comparison between sand–Laponite and sand–bentonite is the behaviour observed during aging. El Mohtar *et al*. (2008) report N_G values of 1% and 1·5% for sand with 3% and 5% bentonite, respectively. These values, which fall within the range typical of sands, are lower than those derived above for sand with Laponite, and are consistent with the smaller values of the creep coefficient reported for the sand–bentonite specimens.

Insights from fabric parameters

Earlier in this paper, it was shown that, for both clean sand and sand–Laponite specimens, the dependence of the shear modulus on void ratio and confining stress (and OCR) was well described by equation (1), which contains two 'fabric parameters': C_g an intrinsic soil constant that depends on the nature of the particles and the fabric; and n, an indicator of the nature of the contacts between the soil particles.

Best fitting each data set as a whole, as is done in Fig. 4(b), the following average values of the fabric parameters are obtained: for clean sand: $C_g = 563$ and $n = 0{\cdot}522$; for sand with 1% Laponite: $C_g = 681$ and $n = 0{\cdot}404$; and for sand with 3% Laponite: $C_g = 552$ and $n = 0{\cdot}562$.

These values are compared in Table 2 to values of C_g and n obtained from three other studies, in which measurements of G_0 were obtained from tests on the same Ottawa sand (ASTM C 778 (ASTM, 2017)) mixed with bentonite (El Mohtar *et al*., 2008), silt (Salgado *et al*., 2000) and kaolin (Carraro *et al*., 2009). Note that the same void ratio function (see equation (2)) was used to normalise the data. This explains deviations between the values of C_g and n shown in the table and those reported in the original publications. In general, it is observed that, as the fine content increases, C_g decreases while n increases – in other words, the stiffness of the composite material is reduced, and the response becomes more stress dependent. The only exception is represented by the data for sand with 1% Laponite. In this case, the increase in C_g (20% relative to the clean sand) and the decrease in n (30% relative to the clean sand) reflect a structure characterised by stiffer particle contacts and more stable grain interactions.

Similar observations can be made when examining the values of α and β, the fabric parameters that describe the relationship between shear velocity and stress level (see equation (4)). Consistent with the lower values of α and the higher values of β measured in clays relative to sands (Cha *et al*., 2014), the addition of 3% Laponite translates into a decrease in α and an increase in β. The opposite is seen with 1% Laponite. This trend is typically observed in cemented sands (Cha *et al*., 2014), suggesting that the Laponite provides some form of bonding at the grain contacts.

Relating response to microstructure

It is proposed that the trends in the dynamic properties described above for specimens with different percentages of Laponite are a direct reflection of the fabric and the interactions at the grain-to-grain contacts. Measurements of the limiting void ratios for sand with 1% and 3% Laponite and the observations of the fabric of sand–Laponite mixtures conducted using optical microscopy provide evidence that in both cases a significant fraction of the Laponite is positioned at and around the contacts between the sand grains. This is a direct result of the strong adhesion between the sand surface and the Laponite that was highlighted by observations with the optical microscope.

The thickness of the clay layer present at the contacts determines the behaviour at very small strains. A relatively

Table 2. Comparison of fabric parameters C_g and n to those obtained in previous studies

Materials	Ottawa sand (ASTM C 778) + Laponite			Ottawa sand (ASTM C 778) + Volclay CP-200 bentonite			Ottawa sand (ASTM C 778) + Sil-Co-Sil 106 silt			Ottawa sand (ASTM C 778) + EPK air-floated kaolin		
Test type	Resonant column			Resonant column			Bender elements			Bender elements		
Stress range	25–300 kPa			25–300 kPa			20–500 kPa			50–400 kPa		
Pre-shear state	Isotropic			Isotropic			Isotropic			Isotropic		
Reference	Present study			El Mohtar *et al.* (2008)			Salgado *et al.* (2000)			Carraro *et al.* (2009)		
		C_g	n		C_g	n		C_g	n		C_g	n
	0%	563	0·522	0%	628	0·519	0%	511	0·453	0%	511	0·453
	1%	681	0·404	3%	509	0·557	5%	386	0·460	2%	516	0·495
	3%	552	0·562	5%	501	0·548	10%	310	0·612	5%	487	0·501
							15%	206	0·772	10%	473	0·508
							20%	190	0·815			

thick Laponite layer (as occurs with a dosage of Laponite of 3% – see Fig. 17(c)) translates into a reduction of the initial shear modulus – that is, Laponite has a softening effect (Fig. 5). This is to be expected, given the compressibility of the Laponite gel formed following hydration of the clay aggregates inside the pore space. However, if the Laponite layer is thin enough (Fig. 17(b)), the modulus of the soil is increased, as a result of the Laponite providing bonding/bridging at the sand grain contacts. This is what is observed with 1% Laponite at all stress levels, and with 3% Laponite at 300 kPa, when the 'excess' Laponite is squeezed out of the contacts.

The presence of Laponite at the contacts and the two reference conditions envisioned above ('thin' as opposed to 'thick' inter-granular layer of Laponite) also explain

(*a*) the increase in D_0 observed relative to clean sand, and the increase in D_0 with increasing Laponite percentage (Fig. 4(d)), as the presence of Laponite at the contacts provides a viscous damping contribution that does not exist for clean sand, and that increases with the amount of clay present
(*b*) the increase in the aging coefficient (N_G) measured with the addition of Laponite (Fig. 8), and the fact that the presence of a 'thick' Laponite layer controls the sensitivity of the soil to aging (evident from the fact that with 3% Laponite the measured values of N_G fall in the range reported for clays).

A few aspects of the behaviour beyond the linear threshold can also be ascribed, at least in part, to the presence of Laponite at the sand grain contacts. In particular, the lower values of damping measured at larger strains ($>\sim$0·01%) in the sand with Laponite relative to clean sand (Fig. 6(b)) may be explained by the Laponite reducing energy dissipation associated with frictional interactions of the sand particles (the dominant source of damping at higher strains).

A number of the observations on the behaviour of sand with Laponite, especially in the non-linear region, cannot instead be explained by the presence of Laponite at the sand grain contacts. An example is the higher delay in generating excess pore pressure in sands with 3% Laponite as opposed to sands with 1% Laponite (Fig. 6(d)). Therefore, it must be concluded that the addition of Laponite enables a second mechanism responsible for reducing particle mobility. It is suggested that this mechanism is the formation in the pore space of a gel-like pore fluid with solid-like properties, as a result of the hydration of the clay present in the pore space. With 1% Laponite, the distribution of the clay is localised at the contacts, and there is not enough clay to allow the formation of a continuous gel across the sand's pore space (Fig. 17(b)). Thus this mechanism might have a secondary, if any, effect. Higher dosages of Laponite enable the formation of the gel throughout the majority of the pore space (Fig. 17(c)), and this second mechanism appears to control the response as the shear strain increases. This explains the extended linear threshold and the delayed excess pore pressure generation and modulus degradation with higher dosages of Laponite (Fig. 6).

SUMMARY AND CONCLUSIONS

This paper has focused on the dynamic properties of a composite material formed by Ottawa sand and silt size aggregates of Laponite, a highly plastic (PI > 1000%) synthetic clay. Undrained resonant column tests were conducted on clean sand specimens and specimens of sand dry-mixed with 1% or 3% Laponite (by dry mass of the sand). Following the set-up, all specimens were flushed with water, back-pressure saturated and isotropically consolidated

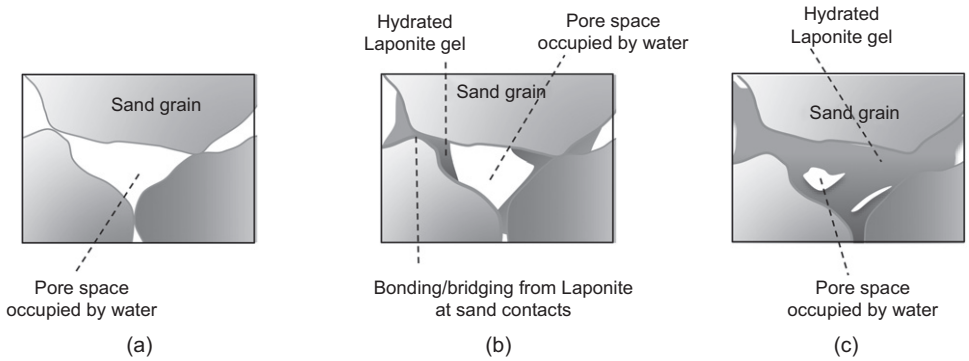

Fig. 17. Summary of hypothesised mechanisms of grain interaction in (a) clean sand and (b), (c) sand with Laponite

to a maximum effective consolidation stress of 100 or 300 kPa. Measurements of the small-strain shear modulus (G_0) and small-strain damping (D_0) were performed throughout the tests to investigate the variation of these properties as a function of stress level and time. Finally, at the maximum consolidation stress, the variations of G and D as a function of shear strain were investigated under undrained conditions.

Despite the small percentages of Laponite considered, significant changes relative to the behaviour of the clean sand were observed in both G_0 and D_0, as well as in the response at higher shear strains. The effect of Laponite on the initial shear modulus (G_0) is dependent on the amount of Laponite present and the consolidation stress.

With 1% Laponite, a significant increase in G_0 relative to the clean sand tested under similar conditions is observed at all confining stresses. Moreover, the soil exhibits reduced stress dependence of the shear modulus compared to clean sand. With 3% Laponite, G_0 exceeds the clean sand value only following consolidation to 300 kPa, and the soil exhibits greater stress level dependency of the shear modulus relative to clean sand.

For both Laponite percentages the small-strain damping ratio, D_0, increases relative to clean sand, with higher values measured with increasing Laponite percentage. Although for the stress range examined, D_0 of clean sand is insensitive to changes in confining stress, for the sand–Laponite specimens, D_0 decreases with an increase in the effective confinement.

The presence of Laponite also affects the evolution of G_0 and D_0 with aging, with significant changes observed in these properties as a function of time. Values of the aging parameter N_G, which quantifies the increase in G_0 with time, increase with Laponite percentage and for 3% Laponite fall in the range of values reported for clays. Also associated with aging is a reduction in D_0.

Regarding the response observed as a function of shear strain, the presence of Laponite translates into an extension of the linear threshold, a delay in the generation of the excess pore pressure, a reduced modulus degradation at any shear strain, relative to the behaviour of clean sand tested under the same conditions. These effects are more evident as the amount of Laponite increases from 1% to 3%. Increasing amounts of Laponite also delay the increase in damping ratio with shear strain, with higher values of D measured on clean sand relative to sand–Laponite measurements beyond $\sim$0·01% strain.

Differences in the fabric of the sand–Laponite specimens and in the particle-to-particle interactions are responsible for the behavioural trends observed in the resonant column tests. While in all cases Laponite interferes with the direct interaction between the sand grains, the amount of Laponite and the applied stress level determine: (*a*) the thickness of the Laponite layer present at the contacts and (*b*) the degree to which the pore space is occupied by the hydrated Laponite.

The first aspect controls primarily the response at small strains. In particular, it is found that a thin clay layer of Laponite provides bonding/bridging at the sand grain contacts, which is responsible for the greater initial shear modulus and the reduced sensitivity of G_0 to the stress level as observed in all tests with 1% Laponite, relative to both clean sand and sand with 3% Laponite. Increases in layer thickness with Laponite dosage also explain the trends of D_0 and sensitivity to aging (as measured by N_G) observed with increasing Laponite percentage.

The second aspect has an impact on the behaviour in the non-linear region, as the formation in the pore space of a pore fluid with solid-like properties is believed to reduce non-linearity and delay excess pore pressure generation. This explains the observed effect of Laponite percentage on linear threshold, modulus degradation and rate of excess pore pressure generation.

ACKNOWLEDGEMENTS

This research was partially funded by the National Science Foundation, Geomechanics and Geotechnical Systems Program, under grant CMS-0928679. Partial funding for the first author was provided by the 'Gestion propia scholarship program' of the National Committee of Science and Technology of Chile (CONICYT), and by Purdue University through the Bilsland Dissertation Fellowship. All support is gratefully acknowledged. Appreciation is extended to Professor Vincent P. Drnevich of Purdue University who provided guidance in interpreting the resonant column test results.

NOTATION

C_g, k, n	non-dimensional soil constants appearing in shear modulus expression
C_u	coefficient of uniformity
$C_{\alpha\varepsilon}$	creep coefficient
D	damping ratio
D_0	initial damping ratio
D_r	relative density
D_{rsk}	skeleton relative density
e	void ratio
e_{min}, e_{max}	limiting void ratios
$e_{minbulk}$, $e_{maxbulk}$	limiting void ratios defined in terms of bulk void ratio
e_{minsk}, e_{maxsk}	limiting void ratios defined in terms of skeleton void ratio
$F(e)$	void ratio function
G	shear modulus
G_0	initial shear modulus
N_G	aging coefficient
P_a	atmospheric pressure
t	time
t_0	aging time at which G/G_0 starts to increase linearly with the logarithm of time
V_s	shear wave velocity
α, β	soil constants appearing in shear wave velocity expression
γ	shear strain
Δu	excess pore pressure
ρ	total density
σ'_{cmax}	maximum effective confining stress
σ'_0	isotropic effective confining stress

REFERENCES

Anderson, D. & Stokoe, K. (1978). Shear modulus: a time dependent soil property. In *Dynamic geotechnical testing: a symposium* (eds M. L. Silver and D. A. Tiedemann), pp. 66–90. Philadelphia, PA, USA: American Society for Testing and Materials.

Anderson, D. & Woods, R. D. (1976). Time-dependent increase in shear modulus of clay. *J. Geotech. Geoenviron. Engng* **102**, No. 5, 525–537.

ASTM (2007). D 4015-07: Standard test methods for modulus and damping of soils by resonant-column method. West Conshohocken, PA, USA: ASTM International.

ASTM (2016a). D 4253-16: Standard test methods for maximum index density and unit weight of soils using a vibratory table. West Conshohocken, PA, USA: ASTM International.

ASTM (2016b). D 4254-16: Standard test methods for minimum index density and unit weight of soils and calculation of relative density. West Conshohocken, PA, USA: ASTM International.

ASTM (2017). C 778-17: Standard specification for standard sand. West Conshohocken, PA, USA: ASTM International.

Balnois, E., Durand-Vidal, S. & Levitz, P. (2003). Probing the morphology of Laponite clay colloids by atomic force microscopy. *Langmuir* **19**, No. 17, 6633–6637.

Baxter, C. & Mitchell, J. (2004). Experimental study on the aging of sands. *J. Geotech. Geoenviron. Engng* **130**, No. 10, 1051–1062.

Bowman, E. & Soga, K. (2003). Creep, ageing and microstructural change in dense granular materials. *Soils Found.* **43**, No. 4, 101–117.

Carraro, J., Prezzi, M. & Salgado, R. (2009). Shear strength and stiffness of sands containing plastic or nonplastic fines. *J. Geotech. Geoenviron. Engng* **135**, No. 9, 1167–1178.

Cascante, G. & Santamarina, J. (1996). Interparticle contact behavior and wave propagation. *J. Geotech. Engng* **9**, No. 10, 831–839.

Cha, M., Santamarina, J. C., Kim, H. S. & Cho, G. C. (2014). Small-strain stiffness, shear-wave velocity, and soil compressibility. *J. Geotech. Geoenviron. Engng* **140**, No. 10: 06014011.

Cho, G. C., Dodds, J. & Santamarina, J. C. (2006). Particle shape effects on packing density, stiffness, and strength: natural and crushed sands. *J. Geotech. Geoenviron. Engng* **132**, No. 5, 591–602.

Dobry, R. & Abdoun, T. (2015). 3rd Ishihara lecture: an investigation into why liquefaction charts work: a necessary step toward integrating the states of art and practice. *Soil Dynamics Earthquake Engng* **68**, 40–56.

Drnevich, V. P., Hardin, B. O. & Shippy, D. J. (1978). Modulus and damping of soils by the resonant-column method. In *Dynamic geotechnical testing: a symposium* (eds M. L. Silver and D. A. Tiedemann), pp. 91–125. Philadelphia, PA, USA: American Society for Testing and Materials.

Duffy, J. & Mindlin, R. D. (1957). Stress stress relations and vibrations of a granular medium. *J. Appl. Mech.* **24**, No. 4, 583–593.

El Howayek, A. (2011). *Characterization, rheology and microstructure of Laponite suspensions.* MSc thesis, School of Civil Engineering, Purdue University, West Lafayette, IN, USA.

El Howayek, A., Bobet, A., Johnston, C. T., Santagata, M. & Sinfield, J. V. (2014). Microstructure of sand-Laponite-water systems using cryo-SEM. In *Proceedings geocongress 2014: geo-characterization and modeling for sustainability* (eds M. Abu-Farsakh, X. Yu and L. R. Hoyos), GSP no. 234, pp. 693–702. Reston, VA, USA: American Society of Civil Engineers.

Ellis, E., Soga, K., Bransby, M. & Sato, M. (2000). Resonant column testing of sands with different viscosity pore fluids. *J. Geotech. Geoenviron. Engng* **126**, No. 1, 10–17.

El Mohtar, C. (2008). *Pore fluid engineering: an autoadaptive design for liquefaction mitigation*. PhD dissertation, School of Civil Engineering, Purdue University, West Lafayette, IN, USA.

El Mohtar, C., Santagata, M., Bobet, A., Drnevich, V. & Johnston, C. (2008). Effect of plastic fines on the small strain stiffness of sand. *Proceedings of the 4th international symposium on deformation characteristics of geomaterials (IS-Atlanta)* (eds S. E. Burns, P. W. Mayne and J. C. Santamarina), pp. 245–251. Amsterdam, the Netherlands: IOS Press.

El Mohtar, C. S., Bobet, A., Santagata, M. C., Drnevich, V. P. & Johnston, C. T. (2013). Liquefaction mitigation using bentonite suspensions. *J. Geotech. Geoenviron. Engng* **139**, No. 8, 1369–1380.

El Mohtar, C. S., Bobet, A., Drnevich, V. P., Johnston, C. & Santagata, M. C. (2014). Pore pressure generation in sands with bentonite: from small strains to liquefaction. *Géotechnique* **64**, No. 2, 108–117, https://doi.org/10.1680/geot.12.P.169.

Goddard, J. D. (1990). Nonlinear elasticity and pressure-dependent wave speeds in granular media. *Proc. R. Soc. A: Math., Phys. Engng Sci.* **430**, No. 1878, 105–131.

Gratchev, I. B., Sassa, K., Osipov, V. I. & Sokolov, V. N. (2006). The liquefaction of clayey soils under cyclic loading. *Engng Geol.* **86**, No. 1, 70–84.

Gratchev, I. B., Sassa, K., Osipov, V. I., Fukuoka, H. & Wang, G. (2007). Undrained cyclic behavior of bentonite-sand mixtures and factors affecting it. *Geotech. Geol. Engng* **25**, No. 3, 349–367.

Ham, A., Wang, J. & Stammer, J. G. (2012). Relationships between particle shape characteristics and macroscopic damping in dry sands. *J. Geotech. Geoenviron. Engng* **138**, No. 8, 1002–1011.

Hardin, B. (1978). The nature of stress strain behavior of soils. In *Earthquake engineering and soil dynamics – proceedings of the ASCE Geotechnical Engineering Division specialty conference, Pasadena, California, USA*, pp. 3–90. New York, NY, USA: American Society of Civil Engineers.

Hardin, B. & Black, W. (1966). Sand stiffness under various triaxial stresses. *J. Soil Mech. Found.* **92**, No. 2, 27–42.

Hardin, B. & Dmevich, V. (1972). Shear modulus and damping in soils: design equations and curves. *ASCE, J. Soil Mech. Found. Div.* **98**, No. 7, 9006–9029.

Herrera, N., Letoffe, J. & Putaux, J. (2004). Aqueous dispersions of silane-functionalized Laponite clay platelets. A first step toward the elaboration of water-based polymer/clay nanocomposites. *Langmuir* **20**, No. 5, 1564–1571.

Hou, W., Zhao, W. A. & Li, D. X. (2004). Synthesis and properties of polystyrene/Laponite nanocomposites. *Chin. J. Polym. Sci.* **22**, No. 5, 459–462.

Hsu, C., Asce, M., Vucetic, M. & Asce, M. (2007). Threshold shear strain for cyclic pore-water pressure in cohesive soils. *J. Geotech. Engng* **132**, No. 10, 1325–1335.

Huang, Y. & Wang, L. (2016). Laboratory investigation of liquefaction mitigation in silty sand using nanoparticles. *Engng Geol.* **204**, No. April, 23–32.

Iwasaki, T. & Tatsuoka, F. (1977). Effects of grain size and grading on dynamic shear moduli of sands. *Soils Found.* **17**, No. 3, 19–35.

Joshi, Y. M., Reddy, G. R., Kulkarni, A., Kumar, N. & Chhabra, R. (2008). Rheological behaviour of aqueous suspensions of Laponite: new insights into the ageing phenomena. *Proc. R. Soc.* **464**, No. 2090, 469–489.

Kokusho, T. (1980). Cyclic triaxial test of dynamic soil properties for wide strain range. *Soils Found.* **20**, No. 2, 45–60.

Kroon, M., Vos, W. L. & Wegdam, G. H. (1998). Structure and formation of a gel of colloidal discs. *Phys. Rev. E* **57**, No. 2, 1962–1970.

Krumbein, W. C. & Sloss, L. L. (1963). *Stratigraphy and sedimentation*, vol. 2, p. 660. San Francisco, CA, USA: Freeman.

Lee, J., Salgado, R. & Carraro, J. (2004). Stiffness degradation and shear strength of silty sands. *Can. Geotech. J.* **41**, No. 5, 831–843.

Lee, C., Suh, H. S., Yoon, B. & Yun, T. S. (2017). Particle shape effect on thermal conductivity and shear wave velocity in sands. *Acta Geotechnica* **12**, No. 3, 615–625.

Lo Presti, D. C. F., Jamiolkowski, M., Pallara, O. & Cavallaro, A. (1996). Rate and creep effect on the stiffness of soils. In *Measuring and modeling time dependent soil behavior* (eds T. C. Sheahan and V. N. Kaliakin), GSP no. 61, pp. 166–180. New York, NY, USA: American Society of Civil Engineers.

Lo Presti, D. C. F., Pedroni, S., Cavallaro, A., Jamiolkowski, M. & Pallara, O. (1997). Shear modulus and damping of soils. *Géotechnique* **47**, No. 3, 603–617, https://doi.org/10.1680/geot.1997.47.3.603.

Mancuso, C., Vassallo, R. & d'Onofrio, A. (2002). Small strain behavior of a silty sand in controlled-suction resonant column torsional shear tests. *Can. Geotech. J.* **39**, No. 1, 22–31.

Marcuson, W. I. & Wahls, H. E. (1978). Effects of time on damping ratio of clays. In *Dynamic geotechnical testing: a symposium* (eds M. L. Silver and D. A. Tiedemann), pp. 126–147. Philadelphia, PA, USA: American Society for Testing and Materials.

Michalowski, R. & Nadukuru, S. (2012). Static fatigue, time effects, and delayed increase in penetration resistance after dynamic compaction of sands. *J. Geotech. Geoenviron. Engng* **138**, No. 5, 564–574.

Nakagawa, K., Soga, K., Mitchell, J. K. & Sadek, M. S. (1995). Soil structure changes during and after consolidation as indicated by shear wave velocity and electrical conductivity measurements. *Proceedings of the international symposium on compression and consolidation of clayey soils* (eds O. Kusakabe and H. Yoshikuni), vol. 2, pp. 1069–1074. Rotterdam, the Netherlands: A. A. Balkema.

Ochoa-Cornejo, F., Bobet, A., Johnston, C. T., Santagata, M. & Sinfield, J. (2014). Liquefaction 50 years after Anchorage 1964; how nanoparticles could help prevent it. *Proceedings of the 10th national conference in earthquake engineering: frontiers of earthquake engineering*, Anchorage, AK, USA.

Ochoa-Cornejo, F., Santagata, M., Bobet, A., Johnston, C. T. & Sinfield, J. V. (2016). Cyclic behavior and pore pressure generation in sands with Laponite, a super-plastic nanoparticle. *Soil Dynamics Earthquake Engng* **88**, No. 9, 265–279.

Ochoa-Cornejo, F., Bobet, A., El Howayek, A., Johnston, C. T., Santagata, M. & Sinfield, J. V. (2017). On: Laboratory investigation of liquefaction mitigation in silty sand using nanoparticles [*Engng Geol*. 204: 23–32]. Discussion on 'Laboratory investigation of liquefaction mitigation in silty sand using nanoparticles'. *Engng Geol.* **216**, No. 1, 161–164.

Ovando-Shelley, E. & Pérez, B. E. (1997). Undrained behaviour of clayey sands in load controlled triaxial tests. *Géotechnique* **47**, No. 1, 97–111, https://doi.org/10.1680/geot.1997.47.1.97.

Qiu, T. (2010). Analytical solution for Biot flow–induced damping in saturated soil during shear wave excitations. *J. Geotech. Geoenviron. Engng* **136**, No. 11, 1501–1508.

Rockwood Additives (2008). *Laponite performance additives. Specification sheets*. Widnes, UK: Rockwood Additives Ltd.

Richart, F. E., Hall, J. R. & Woods, R. D. (1970). *Vibrations of soils and foundations*. Englewood Cliffs, NJ, USA: Prentice Hall.

Salgado, R., Bandini, P. & Karim, A. (2000). Shear strength and stiffness of silty sand. *J. Geotech. Geoenviron. Engng* **126**, No. 5, 451–462.

Santagata, M. & Kang, Y. I. (2007). Effects of geologic time on the initial stiffness of clays. *Engng Geol.* **89**, No. 1–2, 98–111.

Santagata, M., Germaine, J. & Ladd, C. (2005). Factors affecting the initial stiffness of cohesive soils. *J. Geotech. Geoenviron. Engng* **131**, No. 4, 430–441.

Santagata, M., Bobet, A., El-Howayek, A., Ochoa-Cornejo, F., Sinfield, J. V. & Johnston, C. T. (2014). Building a nanostructure in the pore fluid of granular soils. In *Geomechanics from micro to macro* (eds K. Soga, K. Kumar, G. Biscontin and M. Kuo), pp. 1377–1383. London, UK: Taylor & Francis Group.

Santamarina, J., Klein, K. & Fam, M. (2001). *Soils and waves: particulate materials behavior, characterization and process monitoring*. New York, NY, USA: J. Wiley & Sons.

Sawangsuriya, A. (2012). Wave propagation methods for determining stiffness of geomaterials. In *Wave processes in classical and new solids* (ed. P. Giovine), pp. 157–200. London, UK: InTech.

Sawangsuriya, A., Fratta, D., Bosscher, P. J. & Edil, T. B. (2007). S-wave velocity-stress power relationship: packing and contact behavior of sand specimens. In *Advances in measurement and modeling of soil behavior* (eds D. J. DeGroot, C. Vipulanandan, J. A. Yamamuro, V. N. Kaliakin, P. V. Lade, M. Zeghal, U. El Shamy, N. Lu and C. R. Song), vol. GSP no. 173, pp. 1–10. Reston, VA, USA: American Society of Civil Engineers.

Saxena, S. K., Avramidis, A. S. & Reddy, K. R. (1987). Dynamic moduli and damping ratios for cemented sands at low strains. *Can. Geotech. J.* **25**, No. 2, 353–368.

Schmertmann, J. (1991). The mechanical aging of soils. *J. Geotech. Engng* **117**, No. 9, 1288–1330.

Thevanayagam, S., Shenthan, T., Mohan, S. & Liang, J. (2002). Undrained fragility of clean sands, silty sands, and sandy silts. *J. Geotech. Geoenviron. Engng* **128**, No. 10, 849–859.

Viggiani, G. & Atkinson, J. H. (1995). Stiffness of fine-grained soil at very small strains. *Géotechnique* **45**, No. 2, 249–265, https://doi.org/10.1680/geot.1995.45.2.249.

Vucetic, M. & Dobry, R. (1991). Effect of soil plasticity on cyclic response. *J. Geotech. Engng* **117**, No. 1, 89–107.

Vucetic, M., Lanzo, G. & Doroudian, M. (1998). Damping at small strains in cyclic simple shear test. *J. Geotech. Geoenviron. Engng* **124**, No. 7, 585–594.

Wang, Y. H. & Santamarina, J. C. (2007). Attenuation in sand: an exploratory study on the small-strain behavior and the influence of moisture condensation. *Granular Matter* **9**, No. 6, 365–376.

Wang, Y. H. & Tsui, K. Y. (2009). Experimental characterization of dynamic property changes in aged sands. *J. Geotech. Geoenviron. Engng* **135**, No. 2, 259–270.

Zhang, J., Andrus, R. & Juang, C. (2005). Normalized shear modulus and material damping ratio relationships. *J. Geotech. Geoenviron. Engng* **131**, No. 4, 453–464.